Unscented Kalman Filtering for Real Time Thermometry During Laser Ablation Interventions

Mohammadamin Soltani-Sarvestani, Stéphane Cotin, Paola Saccomandi

Unscented Kalman Filtering for Real Time Thermometry During Laser Ablation Interventions

M.A. Soltani-Sarvestani, S. Cotin, and P. Saccomandi, *Senior Member, IEEE*

***Abstract*— We present a data-assimilation Bayesian framework in the context of laser ablation for the treatment of cancer. For solving the nonlinear estimation of the tissue temperature evolving during the therapy, the Unscented Kalman Filter (UKF) predicts the next thermal status and controls the ablation process, based on sparse temperature information. The purpose of this paper is to study the outcome of the prediction model based on UKF and to assess the influence of different model settings on the framework performances. In particular, we analyze the effects of the time resolution of the filter and the number and the location of the observations.**

***Clinical Relevance*— The application of a data-assimilation approach based on limited temperature information allows to monitor and predict in real-time the thermal effects induced by thermal therapy for tumors.**

I. Introduction

Laser ablation treatments are becoming popular techniques for minimally invasive tumor treatment, especially in brain, liver, breast, thyroid, liver [1]–[3]. Laser ablation focuses on destroying tumors by locally increasing its temperature. As in all the thermal ablation techniques, the therapeutic temperature (above 60 °C) should cover the whole tissue mass, while spearing the healthy tissue around [4], [5]. For this aim, an accurate system is required to monitor and predict the evolving tissue temperature, in order to adjust the laser power. Several thermometry approaches have been investigated in the last decades [6]. They include magnetic resonance imaging (MRI)-based thermometry (MRTI) and fiber optic sensors [6], [7]. MRTI is already employed for brain tumor laser ablation [8], while fiber optic sensors are mostly at the research stage [9], [10]. Among available fiber optic sensors, fiber Bragg gratings (FBGs) are attractive for thermometry application during thermal treatments of tissues, due to their low invasiveness, biocompatibility, and the possibility to have array of tens sensors in a single fiber.

Regardless the thermometry method, it is crucial to accurately monitor temperature evolution in the real-time and in all the location of the tumor/surrounding tissue with the aim to tune the laser power delivery for obtaining the best and safer therapy outcome. Thermometry systems, especially MRTI, can be affected by physiological motion, limited signal-to-noise ratio, cavitation artifacts [11]. Similarly, simulations of the heat transfer in tissues undergoing thermal therapies suffer from the inaccuracy of patient-specific parameters and cannot account for unpredictable physiological events [12]. However, a heat transfer model combined with the real-time monitoring of the tissue temperature in specific regions would allow to perform a robust estimate of the procedure state. This approach has been suggested for some many other medical applications, [13] and heating modalities, such as high-intensity focused ultrasound (HIFU) [11], radiofrequency and cryoablation [14], as well as to predict temperature during MR-guided thermal therapy in the presence of noise or corrupted data [15].

In this work, we reconstruct the laser-induced temperature distribution in tissue with a data-assimilation Bayesian framework. The predictions of a heat-transfer model based on the bio-heat equation [4] are associated with information retrieved from the FBGs-measured temperature, using an Unscented Kalman Filter (UKF) [16]. Two approaches are used: a standard, state estimation filtering procedure, where only the temperature is evaluated, and a joint-estimation approach (parameter estimation), where uncertain model parameters are also corrected through the filtering loop. Also, we analyze the influence of the sensor's location and time resolution of the filter on the framework performance.

II. Materials and Methods

For controlling the laser-induced temperature change in liver tissue, the heat model is defined in a 2-dimensional environment. In general, the problem is 3-dimensional, where the 3rd dimension describes the penetration property of the laser beam into the tissue [4]. To simplify the approach for a preliminary analysis, we ignore the penetration property and solve it based on the heat distribution over the liver surface. The UKF updates the model parameters are updated according to the temperature prediction.

A. Obtainment of ground truth data

To obtain ground truth data, experiments have been performed on *ex vivo* liver tissue undergoing laser treatment. Details of the setup and trials are described in the previous work of our group [9], [17]. A network of 125 FBG sensors (5 parallel arrays, each embedded with 25 sensors) was used to measure the tissue temperature induced by the laser. The arrays were placed on the liver surface, to accurately control their location with respect to the laser beam. On the same array, distance between consecutive sensors is 1 mm, whereas distance between parallel arrays is 2 mm. Laser treatment was performed for 90 s, with a near-infrared diode laser.

* This project has received funding from the European Research Council (ERC) under the European Union's Horizon 2020 research and innovation programme (Grant agreement No. 759159).

Mohammadamin Soltani-Sarvestani is with the Department of Mechanical Engineering, Politecnico di Milano, 20156 Milano, Italy (e-mail: mohammadamin.soltani@polimi.it);

Stéphane Cotin is with MIMESIS team of Inria and Strasbourg University, Strasbourg, France (e-mail: stephane.cotin@inria.fr);

Paola Saccomandi is with the Department of Mechanical Engineering, Politecnico di Milano, 20156 Milano, Italy (phone: +39 02 2399 8470; e-mail: paola.saccomandi@polimi.it).

B. Problem Hypothesis

The environment of the problem can be considered as a 2-dimensional cubic network as $(X, Y) \in R^{(5,25)}$, each of which is a sensing point equipped with FBG sensors embedded in five fibers. Fig. 1 illustrates the FBG network which is used in our experiments. We suppose that the location of laser beam center is (0,0) and the sensors are indexed based on the laser beam location.

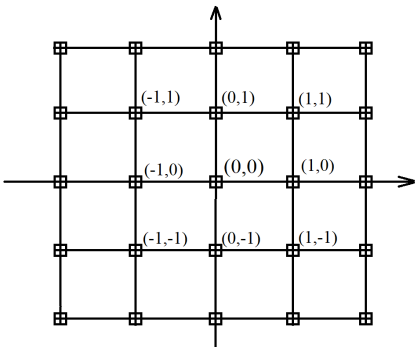

Fig. 1. Installment of the FBG sensors for the experiments. The laser beam is supposed to be located in cartesian coordinates (0, 0), and the sensors are distributed around the laser beam, at different distances.

C. Numerical Model

We consider a 2-dimensional homogeneous heat model which is defined as the following:

$$T_n^{i,j} = T_{n-1}^{i,j} + D^{i,j}\Delta t\left(\frac{T_{n-1}^{i+1,j}+T_{n-1}^{i,j+1}-4T_{n-1}^{i,j}+T_{n-1}^{i-1,j}+T_{n-1}^{i,j-1}}{\Delta x^2}\right) + T_l + \omega^{i+j} \quad (1)$$

where $T_n^{i,j}$ is the temperature of the sensor on the coordinate (x, y) in n^{th} step. T_l is the applied temperature by the laser source, which is calculated as $T_l = \frac{T_{l0}}{\sigma^2} e^{-x_i^2/2\sigma^2}$, $D^{i,j}$ is the tissue diffusivity and Δt is the time resolution of the filter [4], [16]. We consider the value of $q = \frac{T_{l0}}{\sigma^2}$ as stochastic variable in simulations. In addition, we consider a Gaussian error ω^{i+j} for each sensor (or, grating point) considered as ground truth for the model. Also, the difference between the model estimation and the sensor output, which is defined as $T_n^{i,j} = T_n^{FBG_{i,j}} + v^{i,j}$ may affect the model output. We assume fixed (Dirichlet) Boundary Conditions at the grid extremities.

D. Prediction

In the prediction phase, we are estimating $T_n^{i,j}$ in (1) to control the laser power for the laser beam. The Bayesian Filtering (Bayesian Estimation) is a probabilistic method for estimating an unknown probability density function (PDF), recursively. Bayesian filter allows the model to update during the process, and includes two consecutive strategies; prediction and innovation. The parameters that are estimated are: D and q. In this framework, we estimate both the system state and the parameters of the model, and the filter simultaneously updates the system state together with the parameters (joint estimation algorithm). Thus, we compare the results of the parameters estimation (PE, joint estimation) and state estimation (SE) towards the model (1), by using the sparse temperature information provided by the FBG sensors (ground truth, GT). We refer to accuracy as the difference between the temperature estimated by the framework and the ground-truth.

III. Results and Discussion

This section is devoted to demonstrating the efficiency of the proposed Bayesian approach. The simulation starts with the initial values $q = 6\,°C, D = 0.4\,mm^2/s$. Fig. 2 reports the temperature profile measured by the sensors placed on the central array (GT), and the results on one of the outputs of our framework (settings: 25 sensors, the central array in the sensor network, Δt=0.2 s). We can observe that PE provides a temperature trend that is extremely close to the GT. Estimating only the state (SE) drives to low performances for some sensors (the central ones). The model shows low performances across the whole domain.

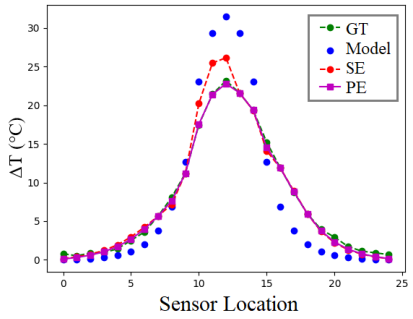

Fig. 2. The comparison between different methods and grand truth. This figure presents the central FBG array in the sensor network.

To analyze the performances of the implemented framework, we compare the accuracy and time complexity of the estimation model using various values for the number and location of observation points chosen to update the model, and Δt. We select different point sets to evaluate the model sensitivity to the number and location of the measurement points (Table I). We select three different reasonable values for Δt such as $\{0.1, 0.2, 0.5\}$. For instance, Δt=0.2 s means that after 5 prediction steps, one correction process is applied over the models' parameters using UKF (the correction step is applied each 1 s).

TABLE I. The selected set points (sensors) around the laser beam to evaluate the sensitivity of UKF model.

SET N.	Selected Sensors
1	(0, -3), (-1, 0)
2	(0,-1),(-1,2)
3	(0, -1), (-1, 0)
4	(0, 2), (2, 0)
5	(0, 3), (-1, 0), (2, 0)
6	(0, 3.),(0, -2),(0, 1)
7	(0, 2), (-1, 0), (2, 0)
8	(0, -4),(0, 3),(0, -2),(0, 1)
9	(0, 4),(0, 3),(0, 2),(0, 1)
10	(0, 2),(0, 1), (-1, 0),(2, 0)
11	(0,-3),(0,2),(0,1),(-1,0),(2,0)
12	(0,4),(0,-3),(0,2),(0,1),(-1,0),(2,0)
13	(0,-5),(0,4),(0,-3),(0,2),(0,1),(-1,0),(2,0)
14	(0,6)(0,-5)(0,4)(0,-3)(0,2)(0,1)(-1,0)(2,0)
15	(0,6),(0,-5),(0,4),(0,-3),(0,2),(0,1),(-1,0),(2,0)
16	(0,-7)(0,6)(0,-5)(0,4)(0,-3)(0,2)(0,1)(-1,0)(2,0)

The results for the central array are presented in Fig. 3.

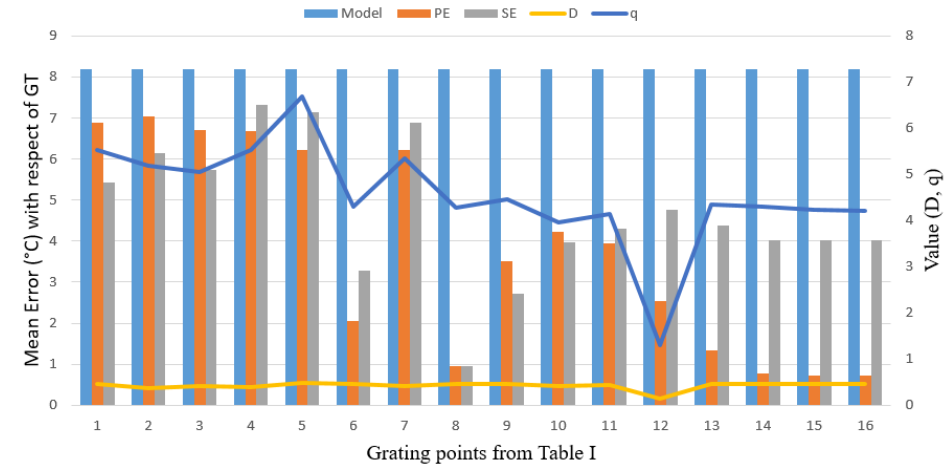

A) Δt=0.1

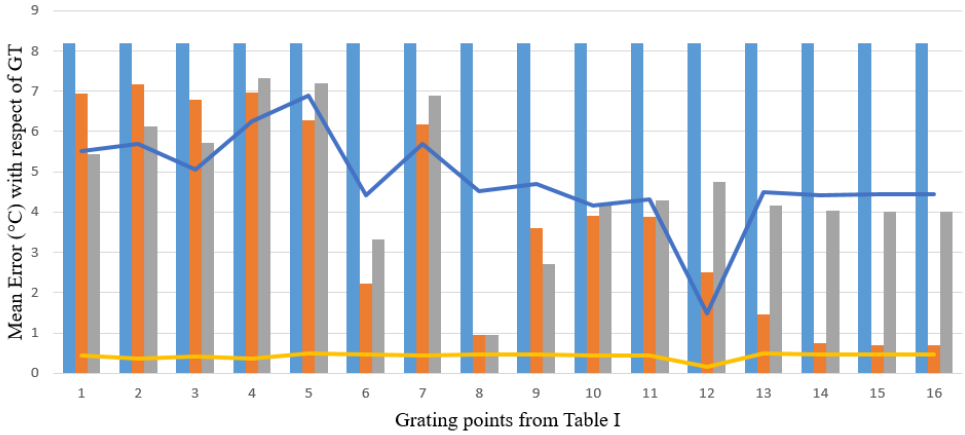

B) Δt=0.2

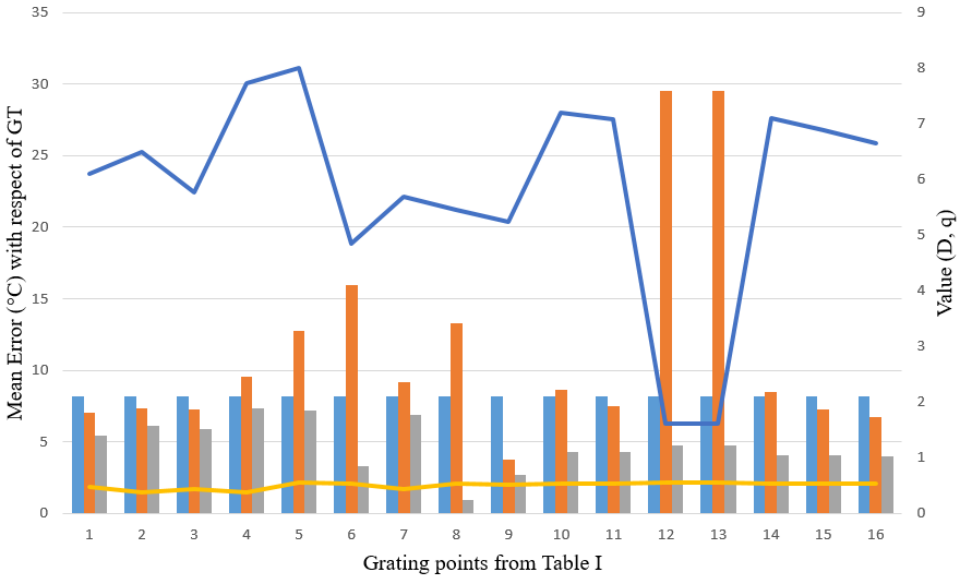

C) Δt=0.5

Fig. 3. The comparison between the models with different number and location of observations and three various values of Δt. The correlation between the results and two model parameters (D and q) are also presented. The figures clearly indicate that the higher number of observations and the lower value of Δt aims better results, with some exceptions.

Fig. 3 presents the results for three different values of Δt. In general, it is clearly visible that lower value of Δt resulted in better predictions, because for higher values of Δt, the correction rate decreased. There is a correlation between the number of sensors and the estimation accuracy (temperature difference between the framework output and the GT). For example, as can be seen in Fig. 3.A and 3.B, the ME of PE for 8 and 9 randomly selected points are less nearly 0.7 °C, because using more point can certainly cover a larger area of the tissue. Using a high number of grating points for UKF correction phase allows obtaining better accuracy. But, as we can see for set number n. 8, with four points, the accuracy is nearly the same as accuracy with eight or nine points. However, by selecting an optimal position for grating points, the number of points is minimized. Because of the limitations in real world problem, such requirement to optimize the grating points is crucial. As a result of this analysis, we suggest applying an optimization solution to select the grating points.

Moreover, a strong correlation between parameters q and D and the mean error cannot be defined. However, when the observations are not selected optimally, the value of D decreases to 0. Since for a biological tissue, D is typically 0.15 mm^2/s [17], [18], we set a threshold to hold the minimum value of D. On the other hand, the value of q tends to increase.

Another considerable parameter in the presented model is the time resolution, Δt. The results with Δt=0.2 s and Δt=0.1 s are nearly the same while their time complexity are different. The time complexity of the model for Δt=0.1 s, 0.2 s, 0.5 s are 15.81 s, 37.41 s and 74.25 s, respectively. Since the sampling duration is 90 s, the model for all examined Δt is working in real-time, but there is trade-off between Δt, accuracy and time complexity which should be carefully considered in practical cases (*e.g.,* during a clinical intervention). The other important factor which is clearly presented in Fig. 3 is the number and the location of observations. Generally, more observations resulted in better performance. While the higher number of observations aims better outcomes, in some point sets better estimations are obtained with less observations. For example, the mean error for PE for the set n. 8, which includes four points, is less than 1.0 °C which is better than results provided by sets n. 9 and n. 10. There is a similar situation for sets n. 5, 6, and 7 with 3 points where the ME for point n. 6 it nearly 2.2 °C which is approximately 3 times better sets n. 5 and 7. We can conclude that there is a strong relationship between the number and location of observations and the accuracy. After a certain number of points, the location is not as important as the location for points in sets with lower number of sensors.

IV. Conclusion

In this study, we analyze the UKF framework for laser ablation monitoring. The UKF model is evaluated against the number of observations (sensors) and the value of Δt. According to our results, there is a strong correlation between the number and location of observations and the accuracy of the estimation. The higher the number of observations, the better the outcome. By lowering the time resolution, UKF is able to better estimate future temperatures, at the expenses of increasing time complexity of the model. The existence of an optimization algorithm to find a trade-off between the number and the sensors location would be beneficial in future studies since there are constraints on the selection of the observations in clinical practice.

Acknowledgment

The authors would like to acknowledge Dr. N. Schulmann for the implementation of the UFK model.

References

[1] D. C. de A. Bastos *et al.*, "The use of laser interstitial thermal therapy in the treatment of brain metastases: a literature review," *https://doi.org/10.1080/02656736.2020.1748238*, vol. 37, no. 2, pp. 53–60, Jul. 2020.

[2] C. M. Pacella *et al.*, "Thyroid tissue: US-guided percutaneous interstitial laser ablation—a feasibility study," *Radiology*, vol. 217, no. 3, pp. 673–677, 2000.

[3] T. de Boorder, L. Waaijer, P. J. van Diest, and A. J. Witkamp, "Ex vivo feasibility study of endoscopic intraductal laser ablation of the breast," *Lasers Surg. Med.*, vol. 50, no. 2, pp. 137–142, Feb. 2018.

[4] P. Saccomandi *et al.*, "Theoretical Analysis and Experimental Evaluation of Laser-Induced Interstitial Thermotherapy in Ex Vivo Porcine Pancreas," *IEEE Trans. Biomed. Eng.*, vol. 59, no. 10, pp. 2958–2964, Oct. 2012.

[5] S. Missios, K. Bekelis, and G. H. Barnett, "Renaissance of laser interstitial thermal ablation," *Neurosurg. Focus*, 2015.

[6] P. Saccomandi, E. Schena, and S. Silvestri, "Techniques for temperature monitoring during laser-induced thermotherapy: An overview," *Int. J. Hyperth.*, vol. 29, no. 7, pp. 609–619, Nov. 2013.

[7] M. De Landro *et al.*, "Fiber bragg grating sensors for performance evaluation of fast magnetic resonance thermometry on synthetic phantom," *Sensors (Switzerland)*, 2020.

[8] J. MacDonell *et al.*, "Magnetic resonance–guided interstitial high-intensity focused ultrasound for brain tumor ablation," *Neurosurg. Focus*, vol. 44, no. 2, p. E11, Feb. 2018.

[9] F. Morra *et al.*, "Spatially resolved thermometry during laser ablation in tissues: Distributed and quasi-distributed fiber optic-based sensing," *Opt. Fiber Technol.*, vol. 58, p. 102295, 2020.

[10] S. Korganbayev *et al.*, "Closed-loop temperature control based on fiber bragg grating sensors for laser ablation of hepatic tissue," *Sensors (Switzerland)*, 2020.

[11] S. Roujol, B. D. de Senneville, S. Hey, C. Moonen, and M. Ries, "Robust adaptive extended Kalman filtering for real time MR-thermometry guided HIFU interventions.," *IEEE Trans. Med. Imaging*, vol. 31, no. 3, pp. 533–542, Mar. 2012.

[12] S. Singh and R. Melnik, "Thermal ablation of biological tissues in disease treatment: A review of computational models and future directions," *https://doi.org/10.1080/15368378.2020.1741383*, vol. 39, no. 2, pp. 49–88, Apr. 2020.

[13] N. Haouchine *et al.*, "Impact of soft tissue heterogeneity on augmented reality for liver surgery," *IEEE Trans. Vis. Comput. Graph.*, vol. 21, no. 5, pp. 584–597, May 2015.

[14] H. Talbot, M. Lekkal, R. Bessard-Duparc, and S. Cotin, "Interactive planning of cryotherapy using physics-based simulation," *Stud. Health Technol. Inform.*, vol. 196, pp. 423–429, 2014.

[15] D. Fuentes, J. Yung, J. D. Hazle, J. S. Weinberg, and R. J. Stafford, "Kalman filtered MR temperature imaging for laser induced thermal therapies," *IEEE Trans. Med. Imaging*, vol. 31, no. 4, pp. 984–994, Apr. 2012.

[16] N. D. Schulmann, M. Soltani-Sarvestani, M. De Landro, S. Korganbayev, S. Cotin, and P. Saccomandi, "Model-Based Thermometry for Laser Ablation Procedure Using Kalman Filters and Sparse Temperature Measurements," *IEEE Trans. Biomed. Eng.*, pp. 1–1, 2022.

[17] A. Mohammadi, L. Bianchi, S. Korganbayev, M. De Landro, and P. Saccomandi, "Thermomechanical Modeling of Laser Ablation Therapy of Tumors: Sensitivity Analysis and Optimization of Influential Variables," *IEEE Trans. Biomed. Eng.*, vol. 69, no. 1, pp. 302–313, Jan. 2022.

[18] L. Bianchi, F. Cavarzan, L. Ciampitti, M. Cremonesi, F. Grilli, and P. Saccomandi, "Thermophysical and mechanical properties of biological tissues as a function of temperature: a systematic literature review," *Int. J. Hyperth.*, vol. 39, no. 1, pp. 297–340, 2022.